



Room temperature deintercalation of alkali metal atoms from epitaxial graphene by formation of charge-transfer complexes

H.-C. Shin, S. J. Ahn, H. W. Kim, Y. Moon, K. B. Rai, S. H. Woo, and J. R. Ahn

Citation: [Applied Physics Letters](#) **109**, 081603 (2016); doi: 10.1063/1.4961633

View online: <http://dx.doi.org/10.1063/1.4961633>

View Table of Contents: <http://scitation.aip.org/content/aip/journal/apl/109/8?ver=pdfcov>

Published by the [AIP Publishing](#)

Articles you may be interested in

[Stacking-dependent electronic property of trilayer graphene epitaxially grown on Ru\(0001\)](#)

Appl. Phys. Lett. **107**, 263101 (2015); 10.1063/1.4938466

[Effect of charge-transfer complex on the energy level alignment between graphene and organic molecules](#)

Appl. Phys. Lett. **100**, 183102 (2012); 10.1063/1.4709428

[Room temperature ferromagnetism in partially hydrogenated epitaxial graphene](#)

Appl. Phys. Lett. **98**, 193113 (2011); 10.1063/1.3589970

[Single-layer metallicity and interface magnetism of epitaxial graphene on SiC \(000 1⁻ \)](#)

Appl. Phys. Lett. **98**, 023113 (2011); 10.1063/1.3543847

[Resonant photoluminescent charging of epitaxial graphene](#)

Appl. Phys. Lett. **96**, 151913 (2010); 10.1063/1.3396201

The image shows the cover of an Applied Physics Reviews journal issue. It features a blue and orange color scheme with a molecular structure background. The text 'NEW Special Topic Sections' is prominently displayed in white. Below it, 'NOW ONLINE' is written in yellow, followed by the title 'Lithium Niobate Properties and Applications: Reviews of Emerging Trends' in white. The AIP Applied Physics Reviews logo is in the bottom right corner.

NEW Special Topic Sections

NOW ONLINE
Lithium Niobate Properties and Applications:
Reviews of Emerging Trends

AIP Applied Physics
Reviews

Room temperature deintercalation of alkali metal atoms from epitaxial graphene by formation of charge-transfer complexes

H.-C. Shin,^{1,a)} S. J. Ahn,^{1,a)} H. W. Kim,¹ Y. Moon,¹ K. B. Rai,¹ S. H. Woo,² and J. R. Ahn^{1,3,b)}

¹Department of Physics, Sungkyunkwan University, Suwon 440-746, South Korea

²College of Pharmacy, Chungnam National University, Daejeon 305-764, South Korea

³SAINT, Sungkyunkwan University, Suwon 440-746, South Korea

(Received 8 June 2016; accepted 13 August 2016; published online 25 August 2016)

Atom (or molecule) intercalations and deintercalations have been used to control the electronic properties of graphene. In general, finite energies above room temperature (RT) thermal energy are required for the intercalations and deintercalations. Here, we demonstrate that alkali metal atoms can be deintercalated from epitaxial graphene on a SiC substrate at RT, resulting in the reduction in density of states at the Fermi level. The change in density of states at the Fermi level at RT can be applied to a highly sensitive graphene sensor operating at RT. Na atoms, which were intercalated at a temperature of 80 °C, were deintercalated at a high temperature above 1000 °C when only a thermal treatment was used. In contrast to the thermal treatment, the intercalated Na atoms were deintercalated at RT when tetrafluorotetracyanoquinodimethane (F4-TCNQ) molecules were adsorbed on the surface. The RT deintercalation occurred via the formation of charge-transfer complexes between Na atoms and F4-TCNQ molecules. *Published by AIP Publishing.*

[<http://dx.doi.org/10.1063/1.4961633>]

Freestanding single-layer graphene with a hexagonally close-packed structure of carbon atoms is a semimetal.^{1,2} Just as the electronic and atomic structures and dimensions of Si are controlled in device applications, those of graphene can also be manipulated by various methods.^{3,4} The energy gap at the Dirac point of graphene was controlled using the stacking order of bilayer or trilayer graphene, the rotational angle of twisted bilayer graphene, graphene nanoribbon, and metal nanostrips.⁵⁻¹¹ The electron or hole doping of graphene was controlled using the adsorption of atoms or molecules and atomic substitution.¹² Furthermore, the two-dimensional graphene developed into a three-dimensional structure.^{13,14} Among various methods to control physical properties of graphene, intercalation and deintercalation have been widely used.¹⁵⁻¹⁹ The electronic structure of graphene grown epitaxially on metal or SiC substrates has been controlled using intercalations of atoms or molecules. Interactions between graphene and substrates and inter-layer interactions between graphene layers have been manipulated by the intercalations.^{20,21} Intercalations have also been used to exfoliate two-dimensional materials.²² Furthermore, recent research on alkali metal ion batteries has intensified the studies on intercalations and deintercalations.^{23,24}

For epitaxial graphene on a SiC substrate, there is an interesting change in electronic structure when atoms or molecules are intercalated. The zero-layer graphene, also known as the buffer layer, has the same atomic structure as single-layer graphene but contains a number of C atoms bonded to the Si atoms in the SiC substrate.²⁵ The zero-layer graphene thus has the insulating flat energy bands.²⁵ When atoms or molecules are intercalated between the zero-layer graphene and the SiC substrate, the zero-layer graphene changes into

single-layer graphene, which results in an insulator-metal transition. To restore the atom (or molecule)-intercalated graphene, the atoms or molecules should be deintercalated. However, deintercalation requires high thermal energy, which is achieved by thermal heating at high temperatures. For example, when Si, Ge, and Y are intercalated between graphene and a SiC substrate, the atoms are deintercalated at 1100, 920, and 700 °C, respectively.^{21,26,27}

Here, we demonstrate that alkali metal atoms can be deintercalated from epitaxial graphene at room temperature (RT) by a molecule acting as an electron acceptor. Na atoms and 2,3,5,6-tetrafluoro-7,7,8,8-tetracyanoquinodimethane (F4-TCNQ) molecules were used as alkali metal atoms and electron-acceptor molecules. First, Na atoms were intercalated between zero-layer graphene and a 6H-SiC(0001) substrate at 80 °C, resulting in electron-doped single-layer graphene. When a thermal treatment was used to deintercalate Na atoms, a high temperature above 1000 °C was required. In contrast to the thermal treatment, F4-TCNQ molecules deintercalated Na atoms at RT. The deintercalation can be interpreted in terms of the formation of charge-transfer complexes between F4-TCNQ molecules (the electron acceptor) and Na atoms (the electron donor). The Na atoms are extracted by the formation of the charge-transfer complexes at the domain boundaries or atomic defects of graphene, resulting in deintercalation. The deintercalation pathways of Na atoms under a thermal treatment at a high temperature can be different from that of the F4-TCNQ-induced deintercalation at RT. The different pathways are because a high thermal energy can make Na atoms deintercalated through various defects, but RT deintercalation induced by F4-TCNQ molecules can happen through limited pathways. The RT deintercalation by the formation of charge-transfer complexes can be applied to an RT chemical sensor based on the change in density of states at the Fermi level.

^{a)}H.-C. Shin and S. J. Ahn contributed equally to this work.

^{b)}Electronic mail: jrahn@skku.edu.

A Si-faced 6H-SiC(0001) substrate was etched at a temperature of 1580 °C under a hydrogen atmosphere in order to cure any polishing damage and obtain flat terraces.^{28,29} After loading the sample into an ultra-high vacuum chamber, it was heated to a temperature of 1150 °C to produce the zero-layer graphene.^{30,31} Na atoms were evaporated from a well-outgassed commercial getter source (SAES) and were deposited on the sample. F4-TCNQ molecules were evaporated from a carbon crucible wrapped with a tungsten wire. The crystalline and electronic structures of the sample were observed using low energy electron diffraction (LEED) and angle-resolved photoemission spectroscopy (ARPES), respectively. The ARPES spectra were measured with a commercial angle-resolved photoelectron spectrometer (R3000, VG-Scienta) and monochromated He-II radiation ($h\nu = 40.8$ eV, VG-Scienta) at RT.

Figure 1 shows the changes in LEED patterns of zero-layer graphene after intercalation and deintercalation. Figure 1(a) is the $(6\sqrt{3} \times 6\sqrt{3})R30^\circ$ LEED pattern of zero-layer graphene produced after heating to a temperature of 1150 °C.^{30,31} The zero-layer graphene has the same atomic structure as single-layer graphene, but a number of carbon atoms in the zero-layer graphene are bonded to the Si atoms in the SiC substrate.²⁵ Na atoms were deposited onto the zero-layer graphene and subsequently heated to a temperature of 80 °C, resulting in the LEED pattern in Figure 1(b). The $(6\sqrt{3} \times 6\sqrt{3})R30^\circ$ LEED pattern disappeared and, consequently, the LEED patterns of graphene and bulk SiC were observed. The disappearance of the $(6\sqrt{3} \times 6\sqrt{3})R30^\circ$ LEED pattern suggests that Na atoms were intercalated between the zero-layer graphene and the bulk SiC. Na atoms might be diffused through domain boundaries or atomic defects of the zero-layer graphene, as reported on intercalations of other atoms or molecules.²⁰ The diffused Na atoms prefer to bond

with the Si atoms of bulk SiC after breaking bonds between the zero-layer graphene and the bulk SiC.^{19,32} The Na intercalations transform the zero-layer graphene into a single-layer graphene.^{19,32} Finally, the single-layer graphene is located on a Na-saturated SiC substrate, as shown in the LEED pattern in Figure 1(b). F4-TCNQ molecules were deposited on the Na-intercalated single-layer graphene at RT. After the RT adsorption of F4-TCNQ molecules, the $(6\sqrt{3} \times 6\sqrt{3})R30^\circ$ LEED pattern reappeared, as shown in Figure 1(c). The reappearance of the $(6\sqrt{3} \times 6\sqrt{3})R30^\circ$ LEED pattern reveals that the intercalated Na atoms were diffused back onto the single-layer graphene, resulting in the transformation of single-layer graphene to zero-layer graphene. The overall intensity of the LEED pattern in Figure 1(c) is lower than that of the LEED pattern in Figure 1(a). A LEED intensity can be reduced when other materials are located on the pathways of the electron diffraction. In this case, because charge-transfer complexes between Na atoms and F4-TCNQ molecules are located on the zero-layer graphene, the overall intensity of the LEED pattern in Figure 1(c) can be lower, compared to that in Figure 1(a). Another possible origin of the reappearance of the $(6\sqrt{3} \times 6\sqrt{3})R30^\circ$ LEED pattern is that the F4-TCNQ molecules form a $(6\sqrt{3} \times 6\sqrt{3})R30^\circ$ superstructure on the single-layer graphene. In this case, however, the intensity of the $(6\sqrt{3} \times 6\sqrt{3})R30^\circ$ LEED pattern should be greater than that of graphene. Furthermore, there is no molecular origin of the superstructure formation and such a molecular superstructure cannot explain the following ARPES intensity maps. As a comparative experiment, we performed LEED experiments of Na deintercalation induced by a thermal treatment, as shown in Figure 1(d). With raising temperature above 300 °C, the $(6\sqrt{3} \times 6\sqrt{3})R30^\circ$ LEED pattern of the zero-layer graphene was gradually recovered. The LEED pattern of the zero-layer graphene was fully recovered at 1100 °C, where Figure 1(d) is the LEED pattern observed after heating at a high temperature of 1100 °C. The LEED experiments show that Na atoms are fully deintercalated above 1100 °C when heated thermally.

The changes in the electronic structures of the zero-layer graphene by the adsorptions of Na atoms and F4-TCNQ molecules were further studied. Figure 2 shows a change in the electronic structure after the intercalation of Na atoms. The ARPES intensity maps were measured along the k_y direction across the \bar{K} point, as shown schematically in the inset of Figure 2(a), where the \bar{K} point is located at $k_y = 0 \text{ \AA}^{-1}$ in the intensity maps. Zero-layer graphene is insulating because a number of carbon atoms in the zero-layer graphene are bonded to the Si atoms in the bulk SiC, as shown in Figure 2(a).^{3,25} The ARPES intensity map in Figure 2(b) corresponds to the LEED pattern in Figure 1(b) that was observed after the adsorption of Na atoms at RT and subsequent heating to a temperature of 80 °C. The ARPES intensity map shows a typical electronic structure of single-layer graphene after the disappearance of the electronic structure of zero-layer graphene.^{19,32} The appearance of the electronic structure of single-layer graphene supports that zero-layer graphene was transformed into a single-layer graphene by the Na intercalation. The Dirac point of the single-layer graphene is located at a binding energy of 1.30 eV, showing that the single-layer

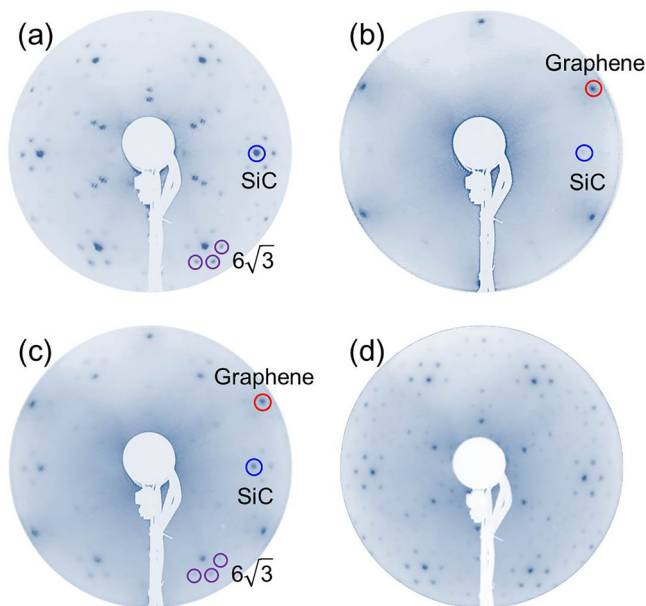


FIG. 1. (a) A LEED pattern of zero-layer graphene on 6H-SiC(0001). (b) A LEED pattern observed after Na atoms were intercalated between the zero-layer graphene and the SiC substrate. (c) A LEED pattern observed after the deposition of F4-TCNQ molecules. (d) A LEED pattern observed after heating at 1100 °C. The LEED spots of bulk SiC, $(6\sqrt{3} \times 6\sqrt{3})R30^\circ$ and graphene are denoted by blue, purple and red circles, respectively.

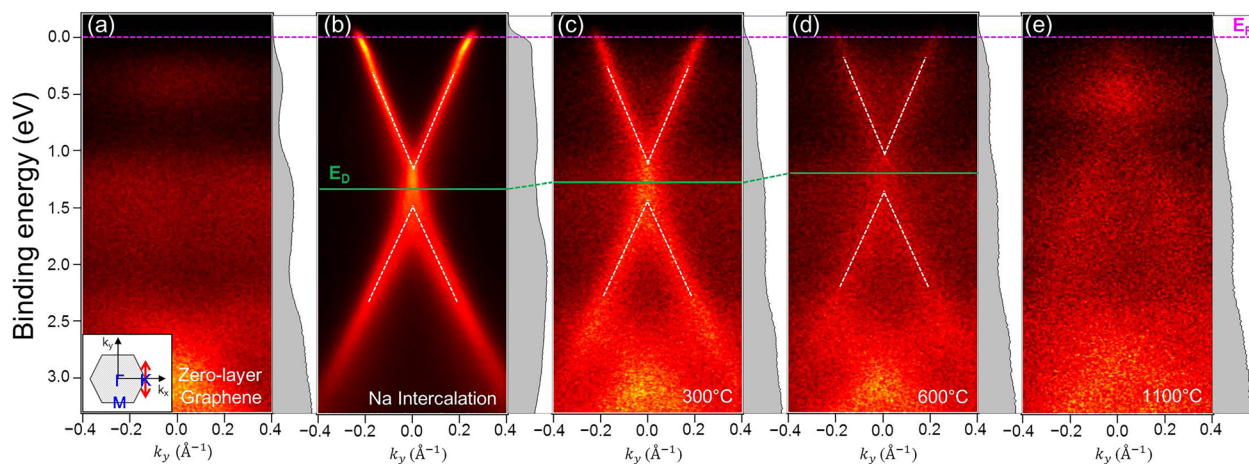


FIG. 2. Changes in the ARPES intensity maps and angle-integrated photoemission spectra of Na-intercalated graphene near the K point. (a) ARPES intensity maps of zero-layer graphene, where its angle-integrated photoemission spectrum is located at the right side. ARPES intensity maps measured (b) after Na intercalation, and after heating to (c) 300, (d) 600, and (e) 1100 °C, respectively. The Dirac points and Fermi level are denoted by green and pink lines, respectively.

graphene is electron-doped. Because the single-layer graphene is located on a Na-covered SiC substrate, electrons are transferred from the intercalated Na atoms.

In general, a finite temperature is required to deintercalate atoms or molecules located between graphene and a substrate. For example, when hydrogen atoms are intercalated, a thermal treatment at a temperature of 900 °C is necessary to deintercalate hydrogen atoms.¹⁹ To understand the thermal stability of the Na-intercalated single-layer graphene, the ARPES intensity maps were measured after increasing the heating temperature. Figures 2(c)–2(e) show the ARPES intensity maps after heating at different high temperatures. The ARPES intensity of single-layer graphene was significantly reduced at temperatures above 600 °C with the reappearance of the electronic structure of zero-layer graphene. The ARPES intensity of single-layer graphene almost disappeared at 1100 °C and only very diffused intensity was observed. This result is consistent with the LEED experiments, where the LEED pattern of the zero-layer graphene is fully recovered at 1100 °C, as shown in Figure 1(d). The changes in the ARPES intensity maps suggest that a high thermal energy corresponding to approximately 1000 °C is required to deintercalate Na atoms, which is much higher than the temperature required for the Na intercalation. The thermal stability reveals that the intercalation and deintercalation processes are different. Further heating to a higher temperature than that of the Na intercalation may cause most of the intercalated Na atoms to produce a compound with higher thermal stability, such as sodium silicide, instead of deintercalation. When Na atoms are intercalated, they are located on the Si-terminated surface of bulk SiC. The reactions between Na atoms and the Si-terminated surface are similar to those of a Na-covered Si(111) surface.³³ When Na atoms are adsorbed on a Si(111)–7 × 7 surface at RT, Na atoms do not disturb the overall structure of the Si(111)–7 × 7 surface. When heated to higher temperatures between 410 and 540 °C, the Na/Si(111)–7 × 7 surface changes into a Na/Si(111)–3 × 1 surface without the desorption of Na atoms. Na atoms are completely removed when heated to a temperature of 800 °C for several minutes.³³ The

Dirac point of single-layer graphene shifted toward a lower binding energy. There are two possible mechanisms for the Dirac point shift. One is that when the number of intercalated Na atoms is reduced, electron doping from Na atoms is also reduced. Another is that after intercalated Na atoms form sodium silicide, the magnitude of electron doping is changed because the interactions between Na atoms and single-layer graphene are different.

To deintercalate Na atoms, F4-TCNQ molecules were used instead of a thermal treatment at high temperature. Figure 3 shows the changes in the ARPES intensity maps by the adsorption of F4-TCNQ molecules on the Na-intercalated single-layer graphene. Here, we note that the F4-TCNQ molecules were deposited at RT without further thermal treatment. The ARPES intensity maps were measured with increasing deposition time at RT. The ARPES intensity of electron-doped single-layer graphene decreased gradually. Subsequently, most of the single-layer graphene was transformed into zero-layer graphene after a deposition time of 15 min. Here, the energy bands of a Na-doped F4-TCNQ film were reported to have binding energies of 1.0 and 1.9 eV, respectively, so that the difference in spectral intensity of the ARPES intensity maps between Figures 3(c) and 2(e) originates from the Na/F4-TCNQ complexes.³⁴ The ARPES intensity maps clearly show that the intercalated Na atoms can be deintercalated at RT using F4-TCNQ molecules. In contrast to the thermal deintercalation of Na atoms, the Dirac point of single-layer graphene did not shift and nearly remained at a binding energy of 1.2 eV, as shown in Figure 3(b). It was reported that the F4-TCNQ molecules act as electron acceptors on graphene.¹⁵ For this reason, when the F4-TCNQ molecules are located on a single-layer graphene, the Dirac point of graphene should shift toward a lower binding energy. The unchanged Dirac point thus suggests that the F4-TCNQ molecules are not located on the single-layer graphene and react with the intercalated Na atoms.

Figure 4 shows the schematic drawing of the Na intercalation and deintercalation processes. As described above, a number of carbon atoms of zero-layer graphene are

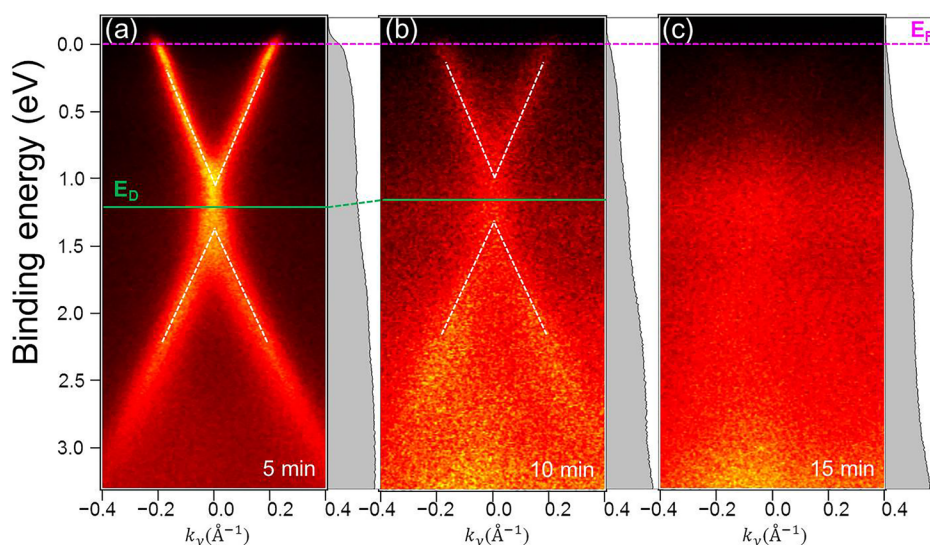


FIG. 3. Changes in ARPES intensity maps and angle-integrated photoemission spectra of Na-intercalated graphene near the K point measured after the deposition of F4-TCNQ molecules for (a) 5, (b) 10, and (c) 15 min at RT.

covalently bonded to the Si atoms of a SiC substrate.^{19,25} Semi-metallic single-layer graphene becomes insulating graphene on a SiC substrate.^{19,25} Most atoms and molecules were reported not to diffuse through the hexagonal rings of graphene because of high energy barriers for diffusion.³ For this reason, atoms and molecules have been reported to be diffused through the domain boundaries between graphene domains or atomic defects within the graphene domains, both of which have low energy barriers for diffusion.²⁰ At a temperature of 80 °C, Na atoms are intercalated between the zero-layer graphene and the SiC substrate. In contrast to the relatively low temperature required for intercalation, Na atoms are deintercalated at a high temperature above 1000 °C. When Na atoms are intercalated, they should break the bonds between the Si atoms on the topmost SiC bilayer and the C atoms of the zero-layer graphene, as shown in Figure 4(a). Subsequently, the Na atoms are bonded to the Si atoms on the topmost SiC bilayer. When the intercalation process is reversible, the heating temperature required for deintercalation should be much lower than that which was measured experimentally. The high deintercalation temperature suggests that the thermal treatment causes the Na atoms on the topmost SiC bilayer to form chemical compounds with higher thermal stability, such as a sodium silicide, before they are deintercalated. Thus, the high deintercalation temperature can originate from the high thermal energy required to dissociate sodium silicide.

In contrast to the thermal deintercalation of Na atoms, when F4-TCNQ molecules were used, the Na atoms were deintercalated at RT, as shown in Figure 4(b). In the case of

the F4-TCNQ molecules, no thermal treatment was used so that the deintercalation process did not produce sodium silicide with a high dissociation energy. The Na atoms can be deintercalated by the electrostatic attractive forces, resulting in the formation of charge-transfer complexes shown in Figure 4(b).^{35–37} The formation of the charge-transfer complexes may occur at the domain boundaries or atomic defects of single-layer graphene, as Na atoms are diffused in the intercalation process. As a result, Na atoms are extracted reversibly and sequentially. When the charge-transfer complexes are formed between the single-layer graphene and the bulk SiC, the electron structure of single-layer graphene should be observed after the adsorption of F4-TCNQ molecules. The charge-transfer complexes should be located on the graphene after the deintercalation of Na atoms, as shown in Figure 4(b). Furthermore, the Dirac point of single-layer graphene was nearly maintained during the deintercalation process. The unchanged Dirac point suggests that Na concentration under the remaining single-layer graphene region is preserved during the deintercalation process. Furthermore, the different behavior of the Dirac points between thermal and F4-TCNQ-induced deintercalation may be related to different deintercalation pathways. Atoms or molecules were reported to be intercalated or deintercalated through defects such as atomic defects or domain boundaries.^{20,26,38} A finite activation energy is thus required to intercalate or deintercalate atoms. When heated thermally, Na atoms can be deintercalated through various defects by a high thermal energy so that Na atoms can be uniformly deintercalated. Subsequently, the uniform deintercalation can induce a gradual change of Na density, resulting

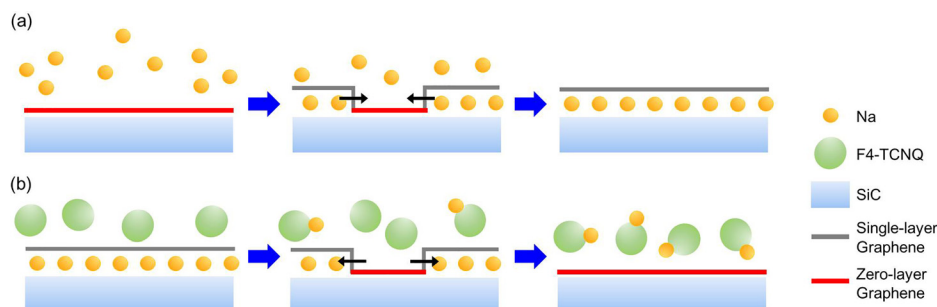


FIG. 4. Schematic side views of (a) Na intercalation process and (b) Na deintercalation process using the F4-TCNQ molecules.

in the change of the Dirac point. In contrast to the thermal deintercalation, the deintercalation induced by F4-TCNQ happens at RT. The pathway of the deintercalation may be limited and similar to that of the intercalation of Na atoms, keeping nearly the same Na density, as shown in Figure 4(b).

In summary, we demonstrated that charge-transfer complexes can be used for RT deintercalation of metal atoms located between graphene and a substrate, whereas a high temperature is required for deintercalation when only thermal treatment is used. The RT deintercalation resulted in reduction in density of states at the Fermi level, where metallic single-layer graphene was transformed into insulating zero-layer graphene. The change in the density of states at the Fermi level was directly observed using ARPES experiments and the change in superstructure was measured using LEED experiments. The change in the density of states at the Fermi level at RT can be applied to an RT chemical sensor based on graphene, which can be used in a gas phase.

This study was supported by a grant from the National Research Foundation of Korea (NRF-2015R1A2A2A01004853) and National Research Foundation of Korea (NRF) grants funded by the Korean Government (MEST) (2015R1A2A2A01002625).

- ¹A. K. Geim and K. S. Novoselov, *Nat. Mater.* **6**, 183 (2007).
- ²K. S. Novoselov, A. K. Geim, S. V. Morozov, D. Jiang, M. I. Katsnelson, I. V. Grigorieva, S. V. Dubonos, and A. A. Firsov, *Nature* **438**, 197 (2005).
- ³A. H. C. Neto, F. Guinea, N. M. R. Peres, K. S. Novoselov, and A. K. Geim, *Rev. Mod. Phys.* **81**, 109 (2009).
- ⁴A. A. Avetisyan, B. Partoens, and F. M. Peeters, *Phys. Rev. B* **81**, 115432 (2010).
- ⁵X. Wang, Y. Ouyang, X. Li, H. Wang, J. Guo, and H. Dai, *Phys. Rev. Lett.* **100**, 206803 (2008).
- ⁶M. Y. Han, B. Özyilmaz, Y. Zhang, and P. Kim, *Phys. Rev. Lett.* **98**, 206805 (2007).
- ⁷Y. Zhang, T.-T. Tang, C. Girit, Z. Hao, M. C. Martin, A. Zettl, M. F. Crommie, Y. R. Shen, and F. Wang, *Nature* **459**, 820 (2009).
- ⁸C. H. Lui, Z. Li, K. F. Mak, E. Cappelluti, and T. F. Heinz, *Nat. Phys.* **7**, 944 (2011).
- ⁹W. Bao, L. Jing, J. Velasco, Y. Lee, G. Liu, D. Tran, B. Standley, M. Aykol, S. B. Cronin, D. Smirnov, M. Koshino, E. McCann, M. Bockrath, and C. N. Lau, *Nat. Phys.* **7**, 948 (2011).
- ¹⁰C. Jeon, H.-C. Shin, I. Song, M. Kim, J.-H. Park, J. Nam, D.-H. Oh, S. Woo, C.-C. Hwang, C.-Y. Park, and J. R. Ahn, *Sci. Rep.* **3**, 2725 (2013).
- ¹¹H.-C. Shin, Y. Jang, T.-H. Kim, J.-H. Lee, D.-H. Oh, S. J. Ahn, J. H. Lee, Y. Moon, J.-H. Park, S. J. Yoo, C.-Y. Park, D. Whang, C.-W. Yang, and J. R. Ahn, *J. Am. Chem. Soc.* **137**, 6897 (2015).
- ¹²M. Papagno, S. Rusponi, P. M. Sheverdyaeva, S. Vlaic, M. Etzkorn, D. Pacilé, P. Moras, C. Carbone, and H. Brune, *ACS Nano* **6**, 199 (2012).
- ¹³Z. Chen, W. Ren, L. Gao, B. Liu, S. Pei, and H.-M. Cheng, *Nat. Mater.* **10**, 424 (2011).
- ¹⁴J.-H. Park, D.-H. Cho, Y. Moon, H.-C. Shin, S.-J. Ahn, S. K. Kwak, H.-J. Shin, C. Lee, and J. R. Ahn, *ACS Nano* **8**, 11657 (2014).
- ¹⁵C. Coletti, C. Riedl, D. S. Lee, B. Krauss, L. Patthey, K. von Klitzing, J. H. Smet, and U. Starke, *Phys. Rev. B* **81**, 235401 (2010).
- ¹⁶A. L. Walter, K.-J. Jeon, A. Bostwick, F. Speck, M. Ostler, T. Seyller, L. Moreschini, Y. S. Kim, Y. J. Chang, K. Horn, and E. Rotenberg, *Appl. Phys. Lett.* **98**, 184102 (2011).
- ¹⁷C. Virojanadara, S. Watcharinyanon, A. A. Zakharov, and L. I. Johansson, *Phys. Rev. B* **82**, 205402 (2010).
- ¹⁸I. Gierz, T. Suzuki, R. T. Weitz, D. S. Lee, B. Krauss, C. Riedl, U. Starke, H. Höchst, J. H. Smet, C. R. Ast, and K. Kern, *Phys. Rev. B* **81**, 235408 (2010).
- ¹⁹C. Riedl, C. Coletti, T. Iwasaki, A. A. Zakharov, and U. Starke, *Phys. Rev. Lett.* **103**, 246804 (2009).
- ²⁰F. Wang, K. Shepperd, J. Hicks, M. S. Nevius, H. Tinkey, A. Tejada, A. Taleb-Ibrahimi, F. Bertran, P. Le Fevre, D. B. Torrance, P. N. First, W. A. de Heer, A. A. Zakharov, and E. H. Conrad, *Phys. Rev. B* **85**, 165449 (2012).
- ²¹K. V. Emtsev, A. A. Zakharov, C. Coletti, S. Forti, and U. Starke, *Phys. Rev. B* **84**, 125423 (2011).
- ²²J. Kim, H. Park, J. B. Hannon, S. W. Bedell, K. Fogel, D. K. Sadana, and C. Dimitrakopoulos, *Science* **342**, 833 (2013).
- ²³E. Yoo, J. Kim, E. Hosono, H.-S. Zhou, T. Kudo, and I. Honma, *Nano Lett.* **8**, 2277 (2008).
- ²⁴A. L. M. Reddy, A. Srivastava, S. R. Gowda, H. Gullapalli, M. Dubey, and P. M. Ajayan, *ACS Nano* **4**, 6337 (2010).
- ²⁵S. Kim, J. Ihm, H. J. Choi, and Y.-W. Son, *Phys. Rev. Lett.* **100**, 176802 (2008).
- ²⁶C. Xia, S. Watcharinyanon, A. A. Zakharov, R. Yakimova, L. Hultman, L. I. Johansson, and C. Virojanadara, *Phys. Rev. B* **85**, 045418 (2012).
- ²⁷S. Watcharinyanon, L. I. Johansson, C. Xia, J. Ingo Flege, A. Meyer, J. Falta, and C. Virojanadara, *Graphene* **2**, 66 (2013).
- ²⁸F. Owman, C. Hallin, P. Mårtensson, and E. Janzen, *J. Cryst. Growth* **167**, 391 (1996).
- ²⁹V. Ramachandran, M. F. Brady, A. R. Smith, R. M. Feenstra, and D. W. Greve, *J. Electron. Mater.* **27**, 308 (1998).
- ³⁰C. Riedl, U. Starke, J. Bernhardt, M. Franke, and K. Heinz, *Phys. Rev. B* **76**, 245406 (2007).
- ³¹C. Riedl, A. A. Zakharov, and U. Starke, *Appl. Phys. Lett.* **93**, 033106 (2008).
- ³²F. Bisti, G. Profeta, H. Vita, M. Donarelli, F. Perrozzi, P. M. Sheverdyaeva, P. Moras, K. Horn, and L. Ottaviano, *Phys. Rev. B* **91**, 245411 (2015).
- ³³S. Olthoff, A. W. McKinnon, and M. E. Welland, *Surf. Sci.* **326**, 113 (1995).
- ³⁴S. Braun and W. R. Salaneck, *Chem. Phys. Lett.* **438**, 259 (2007).
- ³⁵R. Kumai, Y. Okimoto, and Y. Tokura, *Science* **284**, 1645 (1999).
- ³⁶W.-D. Grobman, R. A. Pollak, D. Eastman, E. Maas, Jr., and B. Scott, *Phys. Rev. Lett.* **32**, 534 (1974).
- ³⁷P. D. Josephy, T. Eling, and R. P. Mason, *J. Biol. Chem.* **257**, 3669 (1982).
- ³⁸E. Grañauís, J. Knudsen, U. A. Schroöder, T. Gerber, C. Busse, M. A. Arman, K. Schulte, J. N. Andersen, and T. Michely, *ACS Nano* **6**, 9951 (2012).